International Global Navigation Satellite Systems Society
IGNSS Symposium 2009

Holiday Inn Surfers Paradise, Qld, Australia
1 – 3 December, 2009

Adding Optical Flow into the GPS/INS Integration for UAV navigation

Weidong Ding
School of Surveying and Spatial Information Systems/University of New South Wales/Australia
Phone 61-2-93854202 Fax 61-2-93137493 email weidong.ding@unsw.edu.au
Jinling Wang
School of Surveying and Spatial Information Systems/University of New South Wales/Australia
Phone 61-2-93854203 Fax 61-2-93137493 email jinling.wang@unsw.edu.au
Songlai Han
School of Surveying and Spatial Information Systems/University of New South Wales/Australia
Phone 61-2-93854185 Fax 61-2-93137493 email songlai.han@student.unsw.edu.au
Ali Almagbile
School of Surveying and Spatial Information Systems/University of New South Wales/Australia
Phone 61-2-93854185 Fax 61-2-93137493 email a.almagbile@student.unsw.edu.au
Matthew A. Garratt
School of Aerospace, Civil and Mechanical Engineering/University of New South Wales at the Australian Defence Force Academy Canberra /Australia
Phone 61-2-62688267 Fax 61-2-62688276 email m.garratt@adfa.edu.au
Andrew Lambert
School of Electrical Engineering/Australian Defence Force Academy Canberra /Australia
Phone 61-2-62688351 Fax 61-2-62688443 email a-lambert@adfa.edu.au
Jack Jianguo Wang
School of Electrical, Mechanical and Mechatronic Systems/ University of Technology, Sydney/Australia
Phone 61-2- 95142969 Fax 61-2- 95142655 email jwang@eng.uts.edu.au

ABSTRACT

Autonomously operating unmanned aerial vehicles (UAV) have a great potential for many applications such as reconnaissance, mapping and surveillance. Whilst needing low cost and light weight navigation systems in their implementations, sensors like GPS or low cost inertial sensors can't separately provide either the complete set of information or the required degree of accuracy. Multi-sensor solutions have to be sought to mitigate the shortcomings of individual sensors. Often in such systems, low cost MEMS INS is aided by GPS to provided position, velocity and attitude (PVA) measurements. Data fusion strategies and techniques like extended Kalman filter (EKF) are the kernel for estimating and compensating individual sensor errors to reach improved performance. One drawback of integrating GPS with low cost MEMS INS is the heavy reliance on GPS signal availability. The accuracy of PVA solutions would degrade sharply during GPS signal drop outs due to the poor performance of low cost MEMS INS, which would limit the UAV applications under heavy canopy or city canyon

environments. In some applications like terrain following, integrated GPS/INS system can't provide the ground height which is essential for safety operation in near ground tasks. In this paper, besides integration of GPS and low cost MEMS INS, visual information acquired by a high-resolution CMOS image sensor will be used to augment the PVA estimation. Optical flow rate measurements are used as additional observations in the EKF fusion process. When the ground height is available through an additional sensor like a laser rangefinder (LRF), optical flow rate is used as backup velocity aiding in case of GPS signal drop out. When direct measure of ground height is not available, with velocity from the integrated GPS/INS system, optical flow is used as an effective measure to provide UAV ground height in terrain following tasks. An extended Kalman filter is developed for tightly coupled integration based on the INS psi model which is augmented with optical flow error states. The proposed integration scheme is evaluated with field data collected from real UAV platforms. Both performance improvements and limitations are discussed.

KEYWORDS: GPS, INS, Optical flow, Multi-sensor Integration, Data Fusion.

1. INTRODUCTION

With decreasing costs for sensor and embedded system technologies, the autonomous operating unmanned vehicle (UAV) is becoming very attractive in civil applications such as reconnaissance, mapping and surveillance. Often for on-board navigation and control of such vehicles, the low cost MEMS INS is integrated with GPS to provide a full set of geo-referencing information including position, velocity and attitude (PVA). The measurements from the INS and GPS are mixed using data fusion technologies such as Kalman filter (KF) to generate the optimal PVA solution. One existing drawback of such cost-effective integration of MEMS INS with GPS is the heavy reliance on GPS signal availability. The accuracy of PVA solutions would degrade sharply without GPS aiding due to the poor performance of low cost MEMS INS, which would limit the UAV applications in GPS denied environments. In some applications like terrain following, integrated GPS/INS system can't provide the ground height which is essential for safety operation in near ground tasks.

To overcome the limitations, a number of ways have been investigated to further augment the low cost GPS/INS integrated system, including adding laser range finder, radar, barometer, magnetometer, and vision sensors. Adding vision sensors has become an interesting topic in recent years that attracts many researchers (Corke, 2004; Dissanayake et al., 2001; Kim et al., 2004; Kim and Sukkarieh, 2004; Miura et al., 2002; Winkler et al., 2004). Compared with other spatial sensors, visual sensors have several advantages. It is a self contained and passive sensor which is similar to inertial sensors. This is a very desirable feature when considering the infrastructure cost of using GPS, the fragility of radio and satellite positioning systems in an intentionally signal-jammed environment. In contrast to inertial sensors, it is interactive to the local environment, which enables it to deliver a stable spatial reference with a relatively constant level of accuracy. With the CCD and CMOS imaging sensors, vision sensors can be low cost and very compact which is ideal for UAV applications. Optic flow is a biological inspired technology now being widely accepted for machine vision and automation (Srinivasan, 1994). It detects the motion of visual features across the field of view caused by translation or rotation, since close objects exhibit a higher angular motion in the observer's visual field than distant objects, which has been used to measure the relative range of objects

in the environment.

A number of different approaches have been investigated to apply optic flow measurements in UAV navigation and control (Corke, 2004; Garratt and Chahl, 2008; Wang et al., 2008). Often if ground speed is known, it can be used to calculate the terrain clearance height (here we refer to as ground height); Whilst ground height can be precisely measured with other sensors like a laser range finder (LRF) or ranging radar, optic flow measurements can be used to improve the overall robustness to GPS signal block drop out (Wang et al., 2008).

In the following sections of this paper, an new integration scheme of adding visual information to augment the PVA estimation has been investigated. The visual images are acquired by a high-resolution CMOS camera mounted in the front of the UAV, and the optic flow is calculated using the Image Interpolation Algorithm (I^2A) (Srinivasan, 1994). Then the Optical flow measurements are treated as additional observations in the extended Kalman filter (EKF) fusion process, where the EKF is developed for tightly coupled integration based on the INS psi error model. With such a configuration, the optic flow can be used as an effective measure to provide UAV ground height in terrain following tasks. Mean time, it also acts as a backup aiding to velocity estimation in case of GPS drop out. The proposed scheme has been implemented in a post processing mode and evaluated with the field data collected from a real UAV platform. Both performance improvements and limitations are discussed.

2. ALGORITHMS

2.1 General

The proposed structure of the integrated GPS/INS/Vision navigation system is shown in the following block diagram, see Figure 1. The inertial sensors provide measurements of accelerations and angular rates that are subject to offsets and high noises; the optic flow provides undrifted and noisy estimates of longitudinal and lateral motion rates. GPS provides undrifted position and velocity solutions. The fusion of inertial and optic flow information with GPS measurements is handled in a centralized extended Kalman filter.

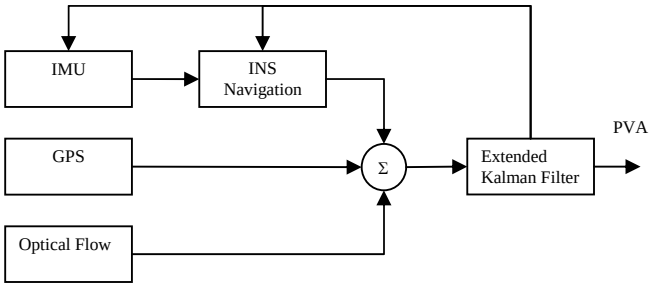

Figure 1. Structure of the integrated GPS/INS/Vision navigation system

2.2 INTEGRATION OF GPS/INS

Considering a multivariable linear discrete system for the integrated GPS/INS system:

$$\mathbf{x}_k = \mathbf{\Phi}_{k-1}\mathbf{x}_{k-1} + \mathbf{w}_{k-1} \tag{1}$$

$$\mathbf{z}_k = \mathbf{H}_k\mathbf{x}_k + \mathbf{v}_k \tag{2}$$

where $\mathbf{x}_k$ is (n×1) state vector,

$\mathbf{\Phi}_k$ is (n×n) transition matrix,

$\mathbf{z}_k$ is (r×1) observation vector,

$\mathbf{H}_k$ is (r×n) observation matrix,

$\mathbf{w}_k$ and $\mathbf{v}_k$ are uncorrelated white Gaussian noise sequences with means and covariances:

$$\begin{aligned} &E\{\mathbf{w}_k\} = E\{\mathbf{v}_k\} = 0 \\ &E\{\mathbf{w}_k\mathbf{v}_i^T\} = 0 \\ &E\{\mathbf{w}_k\mathbf{w}_i^T\} = \begin{cases}\mathbf{Q}_k & i = k \\ 0 & i \neq k\end{cases} \\ &E\{\mathbf{v}_k\mathbf{v}_i^T\} = \begin{cases}\mathbf{R}_k & i = k \\ 0 & i \neq k\end{cases} \end{aligned} \tag{3}$$

Where $E\{\cdot\}$ denotes the expectation function.

$\mathbf{Q}_k$ and $\mathbf{R}_k$ are the covariance matrix of process noise and observation errors, respectively.

Two approaches used for deriving INS error propagation models are well known in the field, namely the perturbation approach and the psi-angle approach(Bar-Itzhack, 1988). In the perturbation error model, the navigation equations are perturbed in the local-level northing-pointing Cartesian coordinate system that corresponds to the true geographic location of the INS; while in the psi-angle error model, the navigation equations are perturbed in the local-level northing-pointing coordinate system that corresponds to the geographic location calculated by the INS. Both models are equivalent and should yield identical results. The psi-angle error is the most widely adopted approach and has been implemented in many tightly coupled integration systems (Da, 1997; Ding, 2008; Grejner-Brzezinska et al., 2005).

$$\begin{aligned} \delta\dot{\mathbf{v}} &= -(\omega_{ie} + \omega_{in}) \times \delta\mathbf{v} - \delta\psi \times \mathbf{f} + \delta\mathbf{g} + \nabla \\ \delta\dot{r} &= -\omega_{en} \times \delta\mathbf{r} + \delta\mathbf{v} \\ \delta\dot{\psi} &= -\omega_{in} \times \delta\psi + \varepsilon \end{aligned} \tag{4}$$

where δv, δr and δψ are the velocity, position, and attitude error vectors respectively;

ω_{ie} is the Earth rate vector;

ω_{in} is the angular rate vector of the true coordinate system with respect to the inertial frame;

ω_{en} is the angular rate vector of the true coordinate system with respect to the Earth;

∇ is the accelerometer error vector;

δg is the error in the computed gravity vector;

ε is the gyro drift vector;
$\mathbf{f}$ is the specific force vector.

For the GPS/INS integration in this work, an INS psi-angle error model has been implemented as the system dynamic model for an extended Kalman filter, with additional state augmentation of INS errors, gravity modelling errors, and lever arm errors. A twenty four state extended Kalman filter is used for data fusion and error estimation, which includes nine navigation solution errors of three dimensional position, velocity and attitude, six accelerometer error modelling parameters (bias and scale factors for each axis), three gyro drifts, three gravity uncertainty errors, and three lever arm errors.

$$\begin{aligned}
\mathbf{x}_{Nav} &= [\delta r_N, \delta r_E, \delta r_D, \delta v_N, \delta v_E, \delta v_D, \delta \psi_N, \delta \psi_E, \delta \psi_D]^T \\
\mathbf{x}_{Acc} &= [\nabla_{bx}, \nabla_{by}, \nabla_{bz}, \nabla_{fx}, \nabla_{fy}, \nabla_{fz}]^T \\
\mathbf{x}_{Gyro} &= [\varepsilon_{bx}, \varepsilon_{by}, \varepsilon_{bz}]^T \\
\mathbf{x}_{Grav} &= [\delta g_N, \delta g_E, \delta g_D]^T \\
\mathbf{x}_{Ant} &= [\delta L_{bx}, \delta L_{by}, \delta L_{bz}]^T
\end{aligned} \tag{5}$$

The complimentary form of extended Kalman filter is used for data fusion (Brown and Hwang, 1997). Its observation vector is the position difference between INS derived position and GPS derived position.

$$\mathbf{z}_k = \mathbf{P}_{INS,k} - \mathbf{P}_{GPS,k} \tag{6}$$

2.3 AUGMENTATION WITH OPTICAL FLOW OBERVATION

A down-looking video camera mounted on the nose part of the UAV is used to measure the optic flow of the ground underneath it. With the assumption that the ground is a flat surface, the optic flow measurement is the sum of translational and rotations portions. When the UAV is moving parallel to the ground surface, the objects observed would shift in the view field. A similar effect exists when the UAV body is tilted. This is true even if the UAV has no translational movement relative to the navigation frame. It is possible to express the optical flow as a combination of translational velocity, rotational velocity and the distance from UAV to the ground surface.

A simplified two dimensional optic flow model has been adopted in this work, where the influence of UAV vertical movement is considered to be trivial. This is reasonable when assuming a UAV is flying over a smooth ground surface at certain height, and assuming there are no high dynamic manoeuvres. The model can be expressed as:

$$Q_x = \frac{V_x}{H} + \omega_y \tag{7}$$

$$Q_y = \frac{V_y}{H} - \omega_x \tag{8}$$

Where Q_x, Q_y are the optic flow measurements.

V_x, V_y are the UAV translational velocities along the camera body axis X and Y.

ω_x, ω_y are the rotational angular rates of the UAV camera.

H is the ground height, which measured from the camera to the ground surface.

From Equations (7) and (8), it is noted that rotation effects have to be subtracted before using optic flow for calculating ground height or translational velocity. Considering both the camera and the INS are rigidly fixed onto the UAV body frame, the rotational angular rates of the UAV camera are substituted using INS gyro measurements in practical calculations.

Equations (7) and (8) would be ill conditioned when ground height becomes very low. To avoid this, a constraint on minimum ground height has to be set in the practical implementation. This is considered to be reasonable because UAV cameras would always be at least a certain height above the ground surface.

The UAV translational velocities used in Equations (7) and (8) are actually longitudinal and lateral velocities of the UAV along the camera body axis X and Y. Again considering both the camera and the INS are rigidly fixed onto the UAV body frame and assuming that the UAV tilt angle is small, for simplification, they are approximated by rotating the UAV velocities in the NED frame

$$\begin{bmatrix} V_x \\ V_y \end{bmatrix} = \begin{bmatrix} \cos(\psi) & \sin(\psi) \\ -\sin(\psi) & \cos(\psi) \end{bmatrix} \begin{bmatrix} V_N \\ V_E \end{bmatrix} \tag{9}$$

Where ψ is the heading angle of the UAV,

V_N, V_D are the UAV north and east velocities under NED frame.

For UAV applications, the ground height H comprises three components:

$$H = H_0 + H_s + H_d \tag{10}$$

Where H_0 is the initial ground height before UAV take-off.

H_s is the height variation of ground surface during UAV flight.

H_d is the height variation due to UAV dynamics.

The initial ground height of the UAV before take-off is a constant value, by differencing Equation (10), we get:

$$\dot{H} = \dot{H}_s - v_d \tag{11}$$

Where v_d is the UAV vertical velocity under the NED frame.

When the optical measurement model of Equations (7) and (8) are perturbed, the error model of optic flow measurements can be written as:

$$\delta Q_x = \frac{\delta V_x}{H} + \delta\omega_y - \frac{V_x}{H^2}\delta H \tag{12}$$

$$\delta Q_y = \frac{\delta V_y}{H} - \delta\omega_x - \frac{V_y}{H^2}\delta H \tag{13}$$

Where $\delta \cdot$ is used to denote error elements.

Substitute Equations (9) and (11) into Equations (12) and (13), and write with state variables in matrix form as:

$$\begin{bmatrix} \delta Q_x \\ \delta Q_y \end{bmatrix} = \begin{bmatrix} \frac{\cos(\psi_D)}{H} & \frac{\sin(\psi_D)}{H} & \frac{\cos(\psi_D)V_N + \sin(\psi_D)V_E}{H^2} & 0 & 1 & 0 & \frac{\cos(\psi_D)V_N + \sin(\psi_D)V_E}{H^2} \\ -\frac{\sin(\psi_D)}{H} & \frac{\cos(\psi_D)}{H} & \frac{-\sin(\psi_D)V_N + \cos(\psi_D)V_E}{H^2} & -1 & 0 & 0 & \frac{-\sin(\psi_D)V_N + \cos(\psi_D)V_E}{H^2} \end{bmatrix} \begin{bmatrix} \delta V_N \\ \delta V_E \\ \delta V_D \\ \delta \omega_x \\ \delta \omega_y \\ \delta \omega_z \\ \delta H_0 \end{bmatrix} \quad (14)$$

In Equation (14), one more state variable is augmented in order to estimate the combined influence of the initial ground height which is a random constant, and the ground surface variation. The observation vector of the EKF is augmented as:

$$\mathbf{z}_k = \begin{bmatrix} \mathbf{P}_{INS,k} - \mathbf{P}_{GPS,k} \\ \delta \mathbf{Q} \end{bmatrix} \quad (15)$$

3. TEST RESULTS

3.1 Test configuration

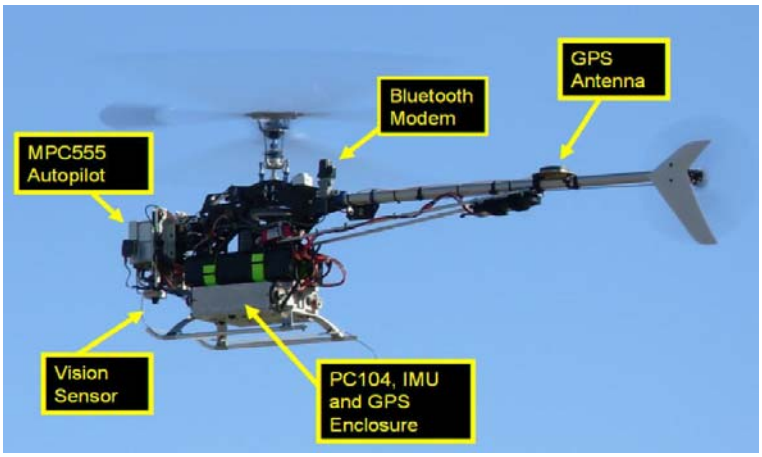

Figure 2. Eagle UAV platform

The UAV used for the field test, see Figure 2, consists of an 8kg helicopter with a microcontroller based autopilot for control and a separate Pentium III processor and frame grabber for vision processing. An in-house made IMU consisting of a sensor cluster with three accelerometers and three gyroscopes has been used. A down looking camera measures the optic flow of the ground underneath the UAV. A GPS mounted on the tail is used to provide position solutions.

For INS body frame, its x-axis points longitudinally forwards of the vehicle, the y-axis laterally towards the right side of the vehicle, and the z-axis vertically downwards completing a right-hand Cartesian coordinate frame. The origin of the INS body frame is not on the

vehicle mass centre. Levararm is defined as the antenna offset vector in the INS body frame.

3.2 Integrated GPS/INS

The first part of the data processing is to implement the integration of GPS with MEMS INS, according to the algorithms introduced in Section 2.2. Figure 3 shows the ground track and height profiles of the test trajectory. The test was carried out in a local area with a range of about 20 meters, and a height of about 2 meters. Figure 4 shows the velocity profiles and Figure 5 the attitudes. A stable estimation of the attitude angles has been achieved with the low cost MEMS INS.

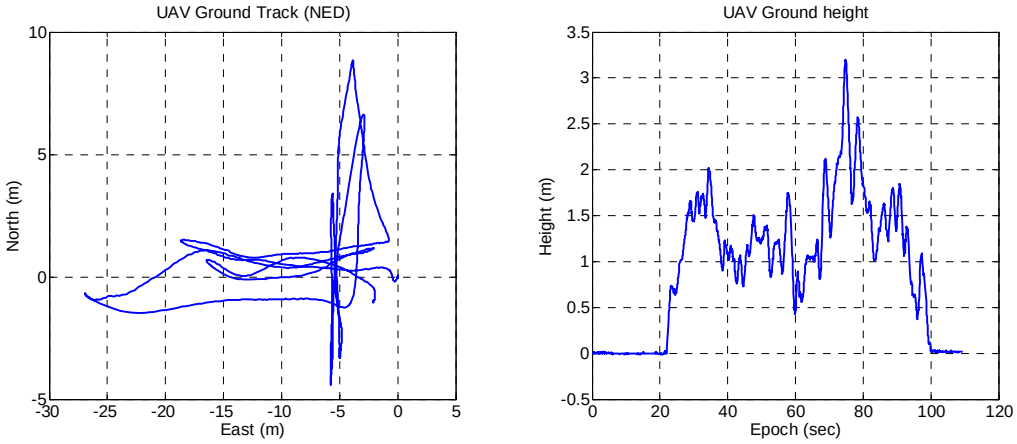

Figure 3. Moving trajectory

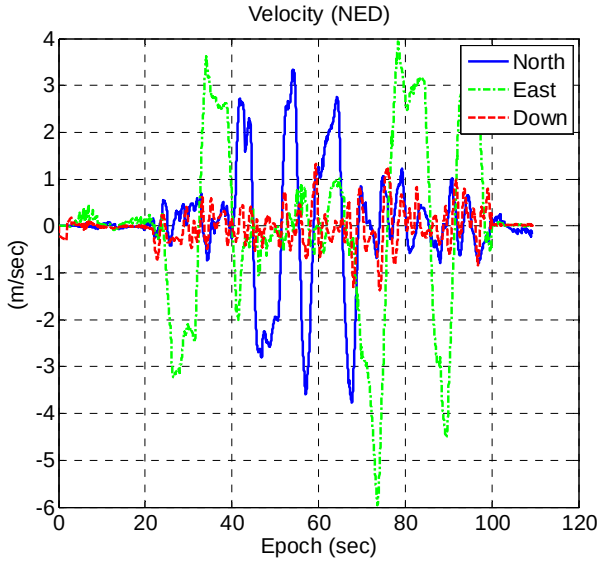

Figure 4. Velocity profiles

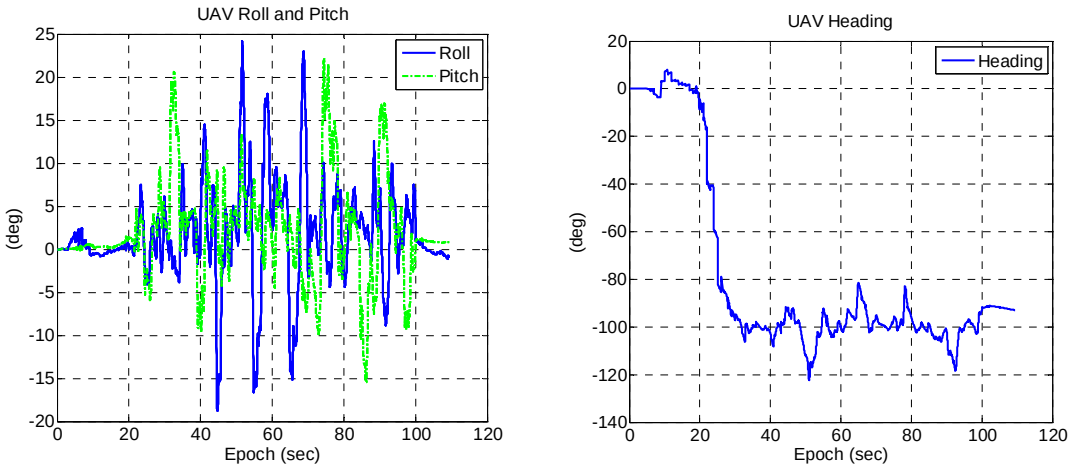

Figure 5. Attitude profiles

3.3 Integrated GPS/INS/Optic Flow

The raw optic flow measurements obtained in the test are very noisy, mainly due to the use of low cost optics, image distortions, un-modelled vibrations of the platform, and simplifications during the modelling stage. Also the low UAV ground speed and height during the test would have caused the increase of the relative noise level. This is easy to see from Equations (7) and (8). To overcome the inherent noise, the raw optic flow measurements were smoothed using a moving average filter comprising five samples before it was used in EKF processing. Figure 6 shows optic flow measurements before and after filtering.

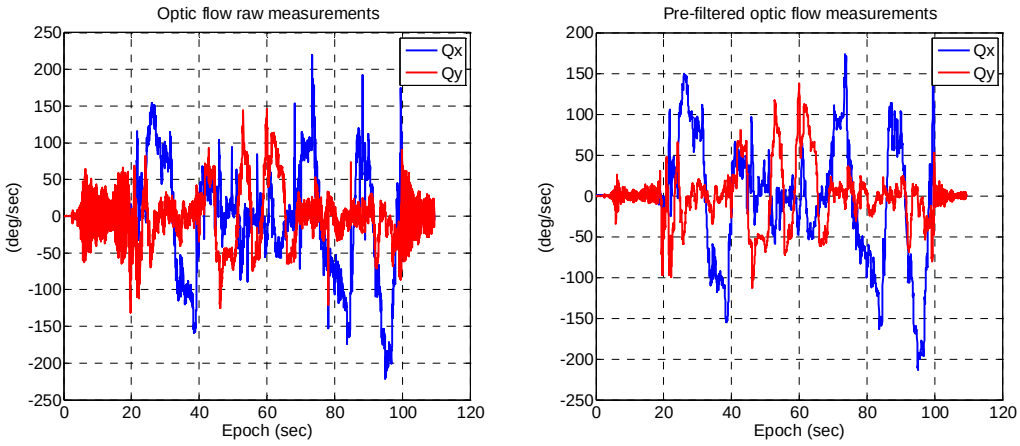

Figure 6. Raw and pre-filtered optic flow measurements

After the EKF was augmented with a ground height error state and optic flow observation vectors, the UAV ground height could be estimated. Figure 7 shows the estimates of ground height, and Figure 8 the EKF estimates of the initial ground height and the RMS errors of the estimated states. The estimation is stable and converged to an RMS accuracy of about 0.1m. A slow drift trend is obvious in the both figures of ground height estimates, and the initial ground height estimates. This can be caused by coloured noises which are not properly modelled in the EKF estimation. Some of the possible error sources have been discussed in previous sections. These error sources need further investigation.

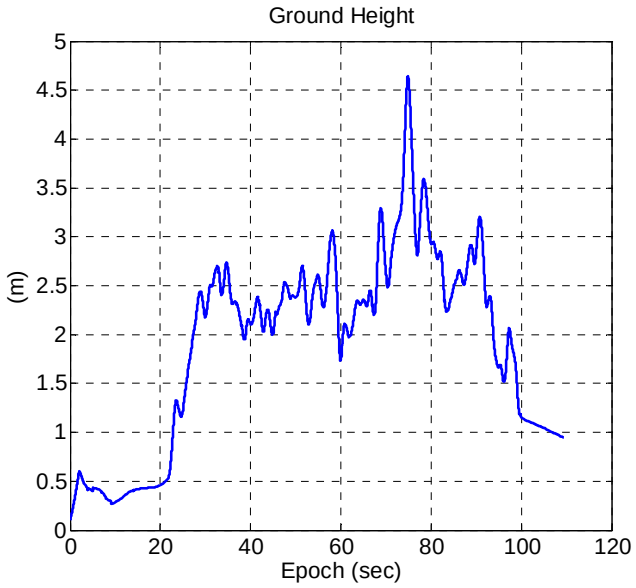

Figure 7. Estimates of ground height

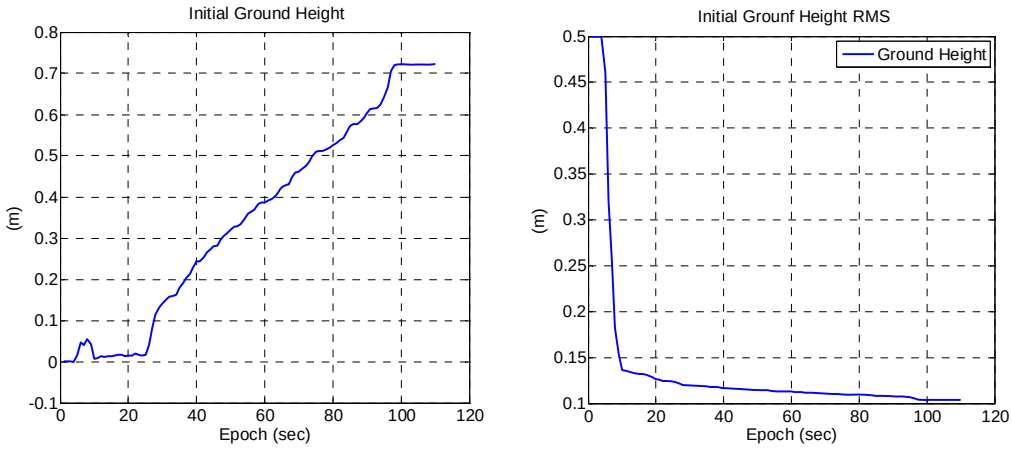

Figure 8. EKF estimates of the initial ground height and the RMS errors of the estimated height

3.4 GPS drop out

To evaluate the benefits of having optic flow aiding, the GPS signals were cut off after the first 60 seconds which left about 50 seconds of GPS drop out period. Then the data set was reprocessed.

With the optic flow and INS measurements, estimation of ground height is still possible even though the estimation error increases quickly. The ground height estimation result has been shown in Figure 9, which can be compared with that in Figure 7. Within the first 20 seconds after GPS drop out, the height estimation error is still within a meter range. After then, the estimation error quickly builds up and goes up in a diverged trend.

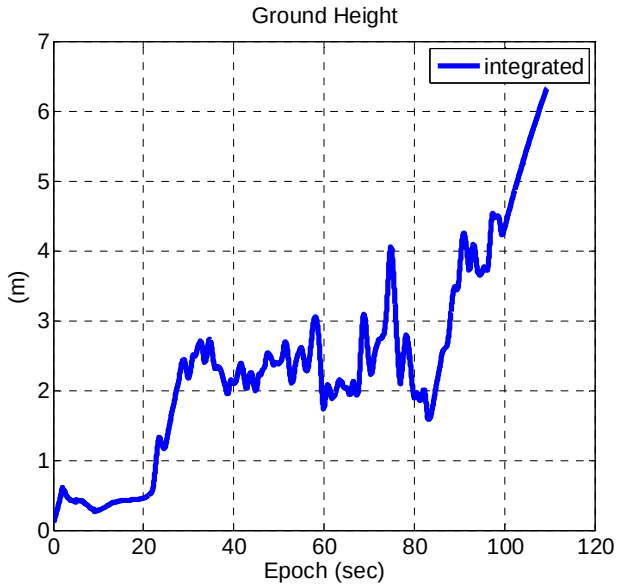

Figure 9. Estimation of ground height after GPS drop out

Figure 10 shows the results of the velocity estimation after GPS dropout. The worst estimation appeared with the velocity in north direction, which has estimation error of about 4m/s at the end of 50 seconds of GPS drop out.

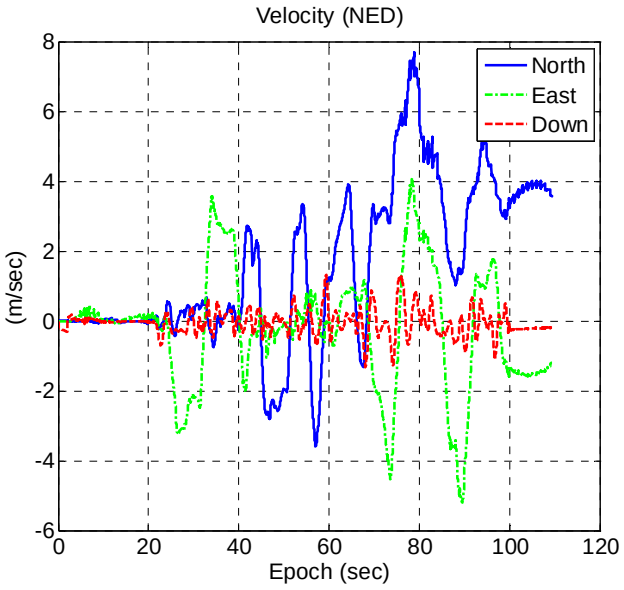

Figure 10. Velocity estimation after GPS drop out

3.5 Both GPS and optic flow drop out

This is the typical scenario with GPS/INS integration when GPS signals are attenuated or totally blocked out. In this scenario, the estimation of ground height becomes impossible. Figure 11 shows the estimation results of the velocities. After about 10 seconds of the GPS drop out, the velocity in the north direction quickly diverged. When compared with Figure 10, it is obvious in the performance improvement of having optic flow aiding.

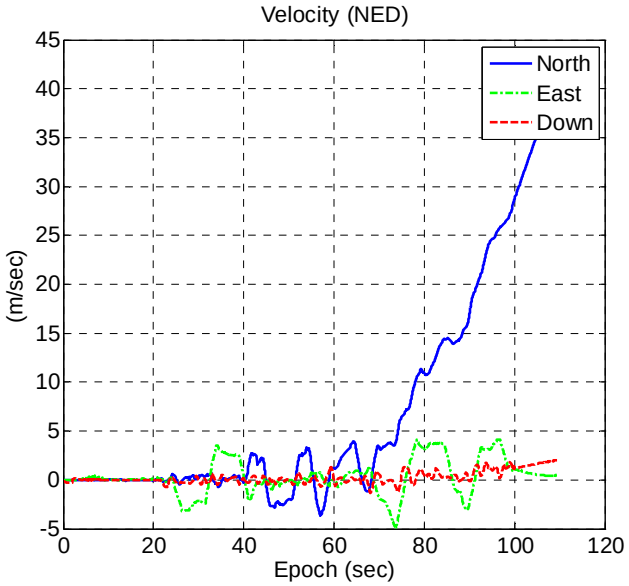

Figure 11. Velocity estimation after both GPS and optic flow drop out

4. CONCLUSING REMARKS

In this work, optic flow measurements obtained from a CCD camera have been used to augment the exiting GPS/MEMS INS integrated system, in the view of improving the overall system availability and providing additional ground height information. To this end, an optic flow measurement error model has been derived and the EKF used for data fusion has been modified to accept more observations, and to have one more state augmented. It has been demonstrated that with such a tight integration configuration the implemented system is capable to estimate the ground height within a reasonable accuracy when all three sensors are working properly. This is essential for UAVs carrying out near ground tasks like terrain following. During GPS signal drop out, the system is still able to maintain a stable solution within a certain period of time with a degraded accuracy. This proves the benefits of adding optic flow to extend the system coasting ability. However, some limitations have also been observed during the data analysis. The optic flow measurements appeared to be very noisy, which could be caused by the imperfection of vision sensor and models used. Also the low speed and low height of the UAV during the test have increased the relative noise level. An unwanted drift in initial ground height estimation will be subject to further investigation. Nevertheless, the overall benefits and performance improvements have been demonstrated.

REFERENCES

Bar-Itzhack, I.Y., Berman, N., 1988. Control theoretic approach to inertial navigation system. AIAA Journal of Guidance, Control & Dynamics, 11(3): 237-245.

Brown, R.G. and Hwang, P.Y.C., 1997. Introduction to random signals and applied Kalman Filtering. John Willey & Sons, New York.

Corke, P., 2004. An inertial and visual sensing system for a small autonomous helicopter. Journal of Robotic Systems, 21(2): 43-51.

Da, R., 1997. Analysis and test results of AIMS GPS/INS system, proceedings of ION GPS-97, Kansas City, USA, pp. 771-780.

Ding, W., 2008. Optimal Integration of GPS with Inertial Sensors: Modelling and Implementation. Ph.D. thesis, University of New South Wales, Sydney.

Dissanayake, M.W.M.G., Newman, P., Clark, S., Durrant-Whyte, H.F. and Csorba, M., 2001. A solution to the simultanenous localization and map building (SLAM) problem. IEEE transactions on robotics and automation, 17(3): 229-241.

Garratt, M.A. and Chahl, J.S., 2008. Vision-Based Terrain Following for an Unmanned Rotorcraft. Journal of Field Robotics, 25(4-5): 284-301.

Grejner-Brzezinska, D., Torh, C. and Yi, Y., 2005. On improving navigation accuracy of GPS/INS systems. Photogrammetric engineering & remote sensing, 71(4): 377-389.

Kim, J., Ridley, M., Nettleton, E. and Sukkarieh, S., 2004. Real-time experiement of feature tracking/mapping using a low-cost vision and GPS/INS system on an UAV platform, The 2004 international symposium on GNSS/GPS, Sydney, Australia.

Kim, J. and Sukkarieh, S., 2004. SLAM aided GPS/INS navigation in GPS denied and unkown environments, The 2004 international symposium on GNSS/GPS, Sydney, Australia.

Miura, J., Itoh, M. and Shirai, Y., 2002. Toward vision-based intelligent navigator: its concept and prototype. IEEE transactions on intelligent transportation systems, 3(2): 136-146.

Srinivasan, M.V., 1994. An image-interpolation technique for the computation of optic flow and egomotion. Biological Cybernetics, 71: 401-415.

Wang, J., Garratt M., Lambert A., Wang J.J., Han S., Sinclair D., 2008. Integration of GPS/INS/Vision sensors to navigate Unmanned Aerial Vehicles, XXI Congress of the Int. Society of Photogrammetry & Remote Sensing, Beijing, P.R. China, pp. 963-970.

Winkler, S., Schulz, H.-W., Buschmann, M., Kordes, T. and Voersmann, P., 2004. Improving low-cost GPS/MEMS-based INS integration for autonomous MAV navigation by visual aiding, ION GNSS 17th International Technical Meeting of the Satellite Division, Long Beach, CA, pp. 21-24.